# Dynamics and bifurcations of a semiconductor laser with short external cavity

B. Krauskopf[a,b], K. Green[a], H. Erzgräber[b], D. Lenstra[b,c]

[a]Department of Engineering Mathematics, University of Bristol, Bristol BS8 1TR, UK
[b]Faculty of Science, Vrije Universiteit Amsterdam, De Boelelaan 1081,
1081 HV Amsterdam, The Netherlands
[c]Research Institute COBRA, Technical University Eindhoven, The Netherlands

## ABSTRACT

We present a theoretical study into the dynamics and bifurcations of a semiconductor laser subject to delayed optical feedback, as modelled by the Lang-Kobayashi equations. For the case of a short external cavity, of the order of a few centimeters, there is a limited number of external cavity modes (ECMs), which makes it possible to apply advanced techniques from dynamical systems, such as the continuation of ECMs and their bifurcations, and the computation of unstable manifolds. From the physical point of view, a short cavity is characterized by the fact that the delay time in the external cavity is of the same order of magnitude as the period of the relaxation oscillation of the laser. In this regime the optical feedback phase is known to play an important role. We provide a detailed overview of how the dynamics depends on the feedback phase, which is in good agreement with recent experimental measurements.

**Keywords:** Semiconductor laser, optical feedback, bifurcation analysis, numerical continuation

## 1. INTRODUCTION

It is well known that even small amounts of delayed optical feedback from a conventional mirror can destabilize a semiconductor laser. Therefore, optical isolators must be used in applications where stable laser operation is needed. On the other hand, semiconductor lasers with feedback are presently considered as possible sources of chaotic carrier waves for communication schemes; see, for example, the recent surveys of Refs. [1–3] as entry points to the extensive literature.

In this paper we consider the case of a short cavity, by which we mean that the round trip time of the external cavity is of the same order of magnitude as the laser's intrinsic relaxation oscillation (which is typically on the order of a few GHz). This case was first introduced in Ref. [4] and was further studied in Ref. [5]; see also Ref. [6]. There are a number of reasons why short cavities are of particular interest. With the integration of optical components, short cavities are now of direct technological importance, while their experimental study has become possible with recent fast measuring technology. Furthermore, short cavities only support a relatively small number of external cavity modes (ECMs), which makes a theoretical analysis much more tractable. At the same time, key dynamical features and bifurcations are already present. There is good reason to believe that the study of short cavities will provide crucial insight into the dynamics of longer cavities.

Our specific interest here is a $2\pi$-periodic bifurcation scenario under variation of the optical feedback phase; detailed in Ref. [5]. Starting from stable laser output one finds a transition to periodic output and then to quasiperiodic power fluctuations before the laser produces irregular output confined within so-called pulse packages. Just before the dynamics suddenly collapses back to stable laser output, these pulse packages become very regular. This highlights the importance of the optical feedback phase for the case of a short cavity. This bifurcation scenario is investigated here theoretically, where we model the system with rate equations as introduced first by Lang and Kobayashi.[7] We then apply advanced tools from bifurcation theory to these model equations, which are mathematically a system of delay differential equations (DDEs).[8–10]

Further author information: (Send correspondence to B. Krauskopf)
E-mail: B.Krauskopf@bristol.ac.uk

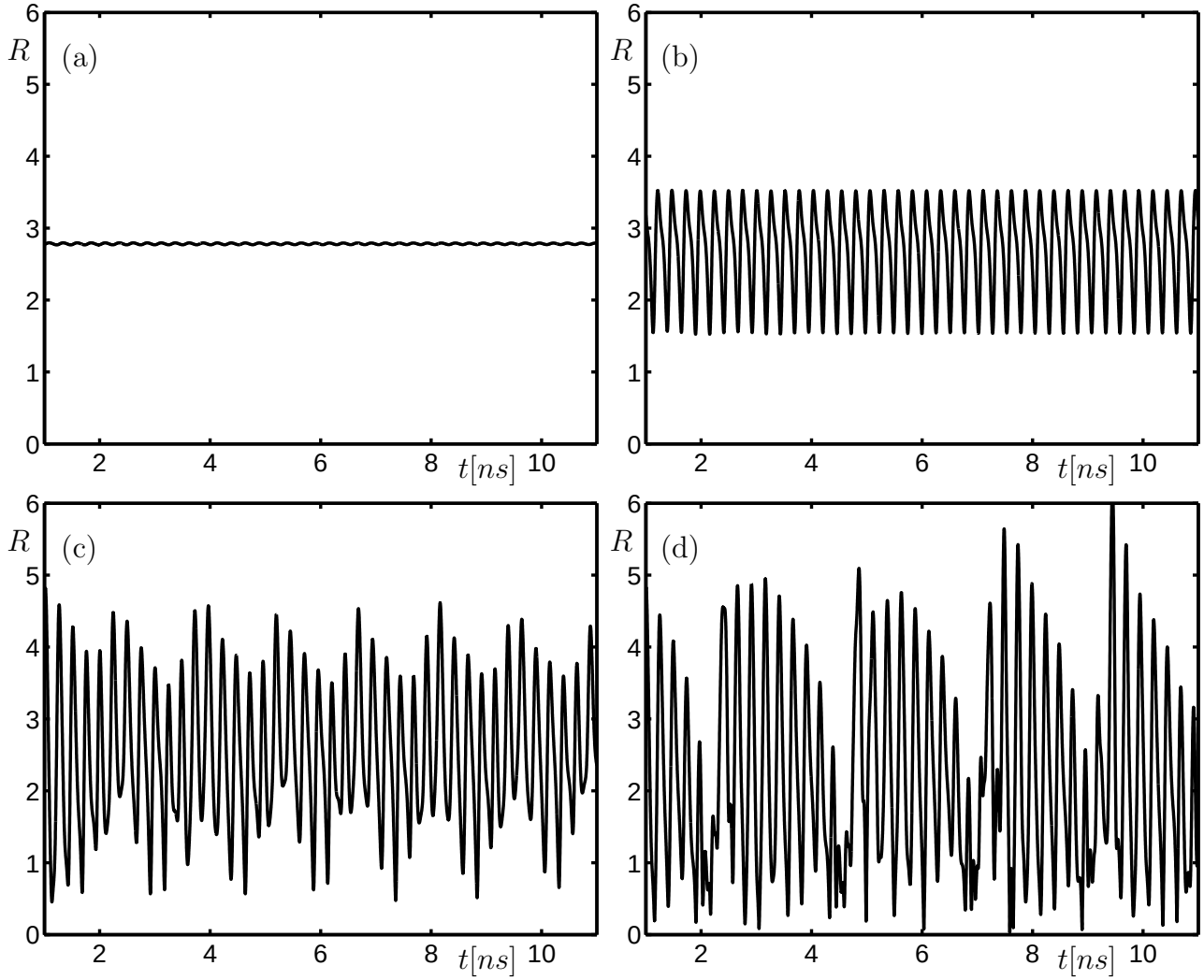


**Figure 1.** Plot of the amplitude $R = |E|$ of the electric field as a function of time. From (a) to (d) the feedback phase $C_p$ takes the values 24.39, 22.74, 21.67, and 20.10.

The paper is organized as follows. In Sec. 2 we introduce the rate equations describing the laser system and discuss some of their basic properties. Section 3 presents a continuation study of the ECMs and bifurcating periodic solutions. In Sec. 4 we present computations of 1D unstable manifolds that explain important global features of the dynamics. Finally, in Sec. 5 we draw some conclusions.

## 2. RATE EQUATIONS

We model the system with the Lang-Kobayashi (LK) equations[7] for the complex electric field $E$ and the inversion $N$ inside the laser, which we write in the form[5]

$$\frac{dE}{dt} = \frac{1}{2} G_{\mathrm{M0}} \left(1 + i\alpha\right) \left(N(t) - N_N\right) E(t) + \kappa E(t-\tau)\, e^{-iC_p} \tag{1}$$

$$\frac{dN}{dt} = J - \gamma_0 N(t) - \left[\Gamma_{\mathrm{M0}} + G_{\mathrm{N0}} \left(N(t) - N_N\right)\right] |E(t)|^2 . \tag{2}$$

Here time is measured in multiples of the carrier lifetime $\gamma$, which was set to $\gamma = 1$ ns. The various physical parameters in these equations are the linewidth enhancement factor $\alpha$, the carrier decay rate $\gamma_0$, the cavity decay

rate $\Gamma_{\mathrm{M0}}$, the feedback strength $\kappa$, the feedback time $\tau$, the quantities $G_{\mathrm{M0}}$ and $G_{\mathrm{N0}}$ are proportional to the small signal gain, the pump current $J$, and the inversion at threshold $N_{\mathrm{N}}$. As in Ref. [5], the parameters are set to the realistic values $\alpha = 3.5,\ \gamma_0 = 1.0,\ \Gamma_{M0} = 0.55,\ \kappa = 25.0,\ \tau = 0.22,\ G_{M0} = 50.0,\ G_{N0} = 0.05,\ J = 8.0,$ and $N_N = 5.0$.

A further and important parameter is the phase $C_p$ of the feedback term in (1). It is given by $C_p = \omega_0\tau$ where $\omega_0$ is the optical frequency of the solitary laser. The phase can be varied by either changing the frequency of the laser (for example, by differing the pump current slightly) or by changing the length of the external cavity on the order of the optical wave length. In both cases all other parameters are essentially unchanged, so that it is justified to consider $C_p$ as an independent parameter in what follows. Note that $C_p$ is a $2\pi$-periodic parameter. Finally, it is important to realize that Eqs. (1)–(2) are invariant under any phase-shift of the complex electric field $E$. One also speaks of an $S^1$-symmetry of Eqs. (1)–(2), where $S^1$ is the group of all rotations of the complex $E$-plane.[11]

Even though Eqs. (1)–(2) model a single-mode laser and neglect the effect of multiple reflections from the external mirror, the LK-equations have been shown, in numerous studies, to agree with experimental measurements in considerable detail. Specifically, for short external cavities, this includes the onset of regular pulse packages.[4] Figure 1 shows four panels of the laser's amplitude $R$ of the electric field (that is, the square root of its output power) as a function of time $t$. Initially, the laser produces light of (nearly) constant intensity (a). When $C_p$ is decreased, periodic oscillations appear (b), which then become quasiperiodic (c). Finally, for even lower $C_p$, the power oscillates irregularly, however, pulse packages with approximately nine pulses per package are clearly seen.

From the mathematical point of view, the LK-equations are a system of DDEs. The fact that DDEs have an infinite-dimensional phase space (the space of continuous functions over the delay interval), means that they are much harder to treat analytically than ordinary differential equations. Nevertheless, in recent years advanced tools from bifurcation theory have been developed for the study of DDEs. In fact, the wish to understand the dynamics and bifurcations of semiconductor lasers with delayed optical feedback has been a considerable motivation behind these developments.[12–14] Specifically, it is now possible to find and follow equilibria and periodic orbits and (some of) their bifurcations in parameters with the package DDE-BIFTOOL.[15] Building on this package, so-called one-dimensional (1D) unstable manifolds of saddle equilibria and periodic orbits can be computed.[16,17] These techniques are employed in this paper to explain a $2\pi$-periodic bifurcation scenario in the parameter $C_p$ that was found experimentally in Ref. [4].

## 3. CONTINUATION OF ECMS

An external cavity mode (ECM) is a solution of Eqs. (1)–(2) of the form

$$(E, N)(t) = (R_s e^{i\omega_s t}, N_s) \tag{3}$$

for constant $R_s$, $\omega_s$ and $N_s$. This type of solution exists because of the $S^1$-symmetry of Eqs. (1)–(2). While an ECM is a perfectly circular periodic orbit in $(E, N)$-space, it corresponds to a single point in the $(R, N)$-plane because $R$ and $N$ do not change. Physically, the laser is producing light of constant intensity.

By inserting Eq. (3) into Eqs. (1)–(2) one can derive a transcendental equation for $\omega_s$ from which $N_s$ and $R_s$ can be computed. In this paper we do not numerically solve this transcendental equation, but find and follow an ECM in the parameter $C_p$ in the full DDE, Eqs. (1)–(2), with the package DDE-BIFTOOL. When plotted in the $(\omega, N)$-plane, the ECMs are discrete points, given by their values of $\omega_s$ and $N_s$, that lie on an ellipse[1]; see Fig. 2(a). When $C_p$ is decreased, two ECMs are born in the low-inversion (high-gain) region in a saddle-node bifurcation and then move up the ellipse. ECMs are destroyed in the high-inversion (low-gain) region in another saddle-node bifurcation. The ECMs shown on the ellipse are for the fixed value of $C_p = 0.0$. The circles correspond to so-called modes, which (near the saddle-node bifurcation in the low-inversion region) are initially stable, and the squares correspond to so-called anti-modes, which are always unstable.

It is important to realise that $\omega_s$ is not a bifurcation parameter itself, but rather a function of $C_p$. How $\omega_s$ depends on $C_p$ is shown in Fig. 2(c). In fact, there is a single curve of $\omega_s$-values, which corresponds to covering the ellipse in Fig. 2(a) infinitely often. One can think of this curve as a single ECM that is continued in $C_p$.

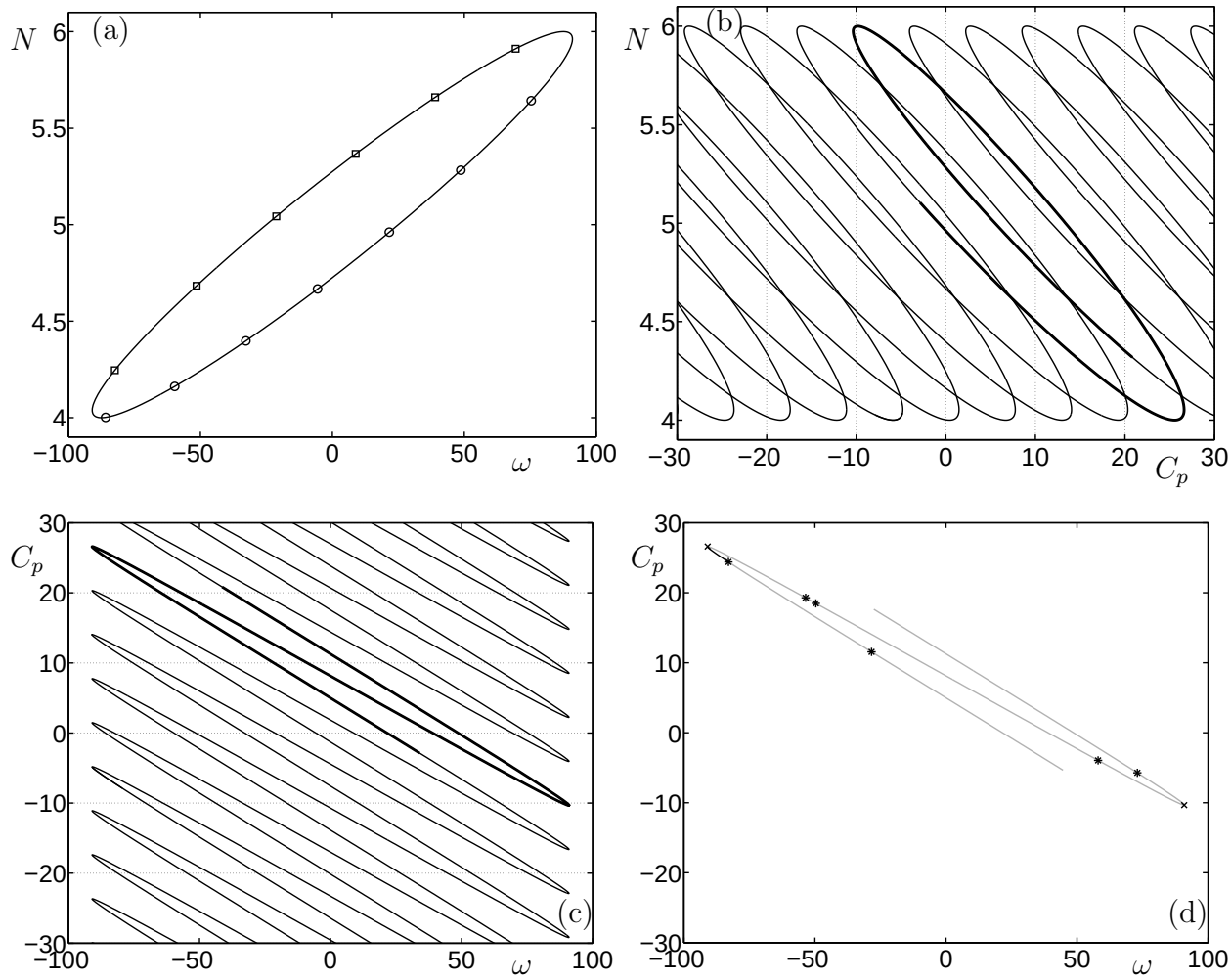


**Figure 2.** The ellipse of ECMs in the $(\omega, N)$-plane (a), the curve of ECMs in the $(C_p, N)$-plane (b) and in the $(\omega, C_p)$-plane (c), and a relevant piece with stability information in the $(\omega, C_p)$-plane (d). The ECMs shown as circles (modes) and squares (antimodes) in panel (a) are for $C_p = 0.0$; saddle-node bifurcations are denoted by $\times$ and Hopf bifurcations by $*$.

The saddle-node bifurcations correspond to the turning points of this curve (as a function of $C_p$). Similarly, the inversion $N_s$ of the ECM is a function of $C_p$ as is shown in Fig. 2(b), again showing a single curve (with self-intersections). Notice the $2\pi$-periodicity in $C_p$ in Figs. 2(b) and (c). Figure 2(d) shows a part of the curve in Fig. 2(c) that covers the ellipse (approximately) once. The curve is now shown with stability information. The black part of the curve corresponds to a stable ECM and grey parts to an unstable ECM. The stability region is bounded on the left by a saddle-node bifurcation ($\times$) and on the right by a Hopf bifurcation ($*$). Further Hopf bifurcations occur on the grey branch where the ECM is already unstable.

We continue the discussion of the ECMs as a function of $C_p$ with Fig. 3 where we plot a relevant part of the ECM curve in the $(C_p, N)$-plane, together with the stability information and branches of periodic solutions computed with DDE-BIFTOOL. Every self-intersection of the curve of ECMs is 'bridged' by a branch of periodic solutions. Such bridges of periodic solutions were first studied in the plane of intensity versus feedback strength in Refs. [18, 19], and they also appear here as a function of the feedback phase $C_p$. There are infinitely many self-intersections and, hence, infinitely many bridges of periodic solutions. However, taking the $2\pi$-symmetry into account, there are exactly three different branches of periodic solutions.

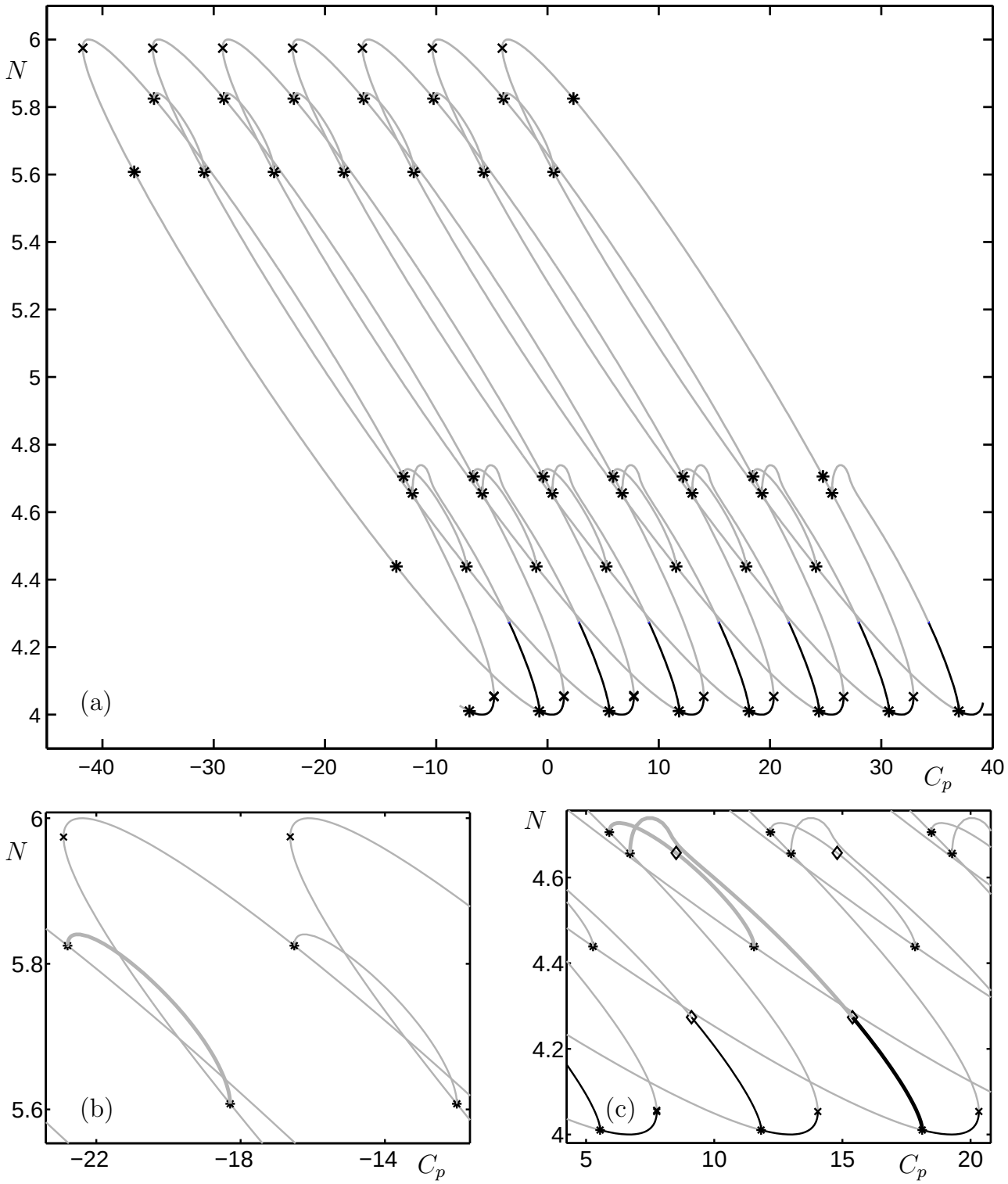


**Figure 3.** A relevant piece of the curve of ECMs with stability information in the $(C_p, N)$-plane, together with branches of periodic solutions bifurcating from Hopf bifurcation points. Saddle-node bifurcations are denoted by $\times$, Hopf bifurcations by $*$, and torus bifurcations by $\diamond$.

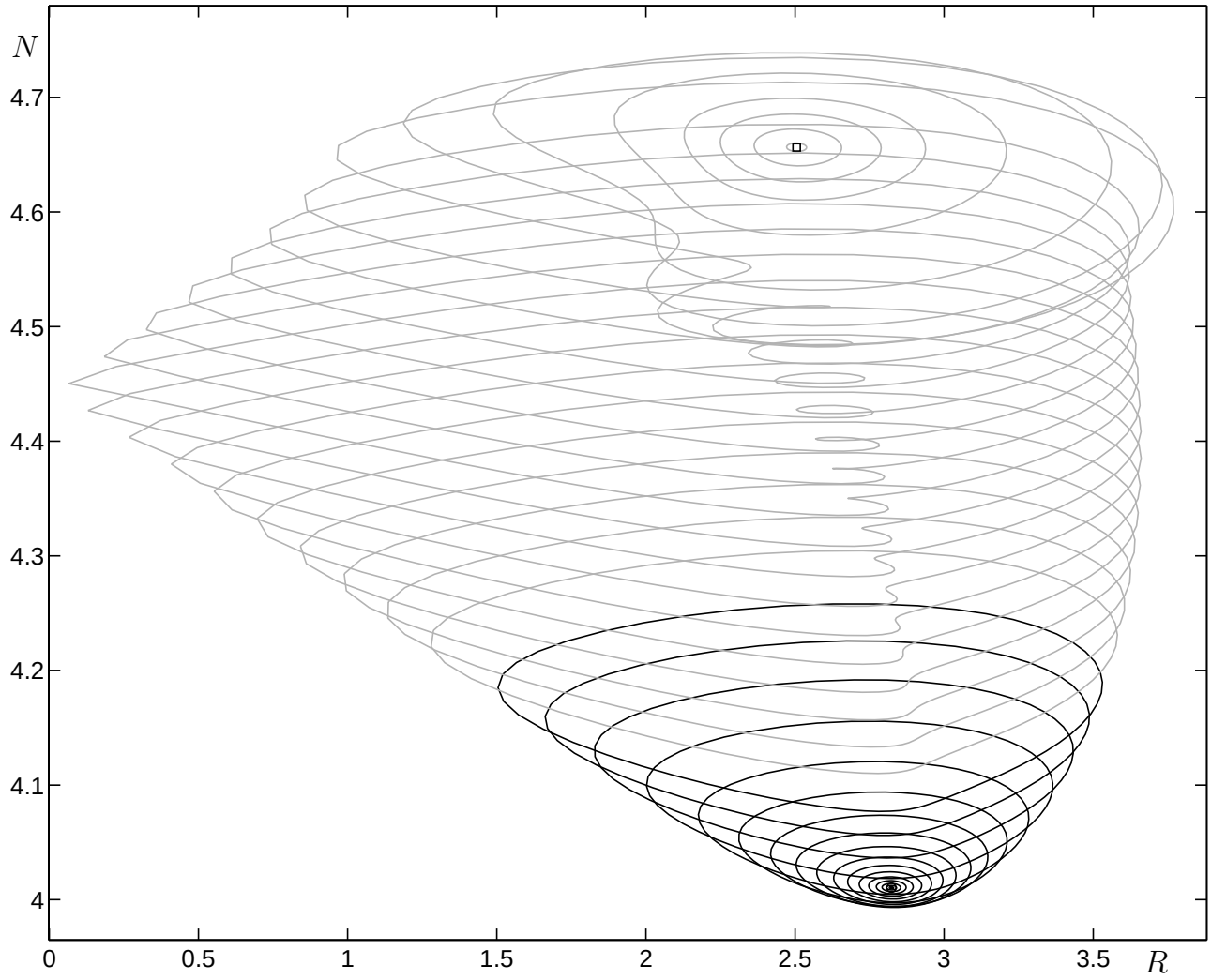


**Figure 4.** Periodic orbits, plotted in projected onto the $(R, N)$-plane, along the branch starting at the boundary of the region of stable ECMs in Fig. 3(b). The black periodic orbits are stable and the gray ones are unstable.

The branch that bridges the self-intersection for $N \approx 5.7$ is shown enlarged and highlighted in Fig. 3(b). The periodic solutions are unstable along this entire branch. The branch bridging the next self-intersection for $N \approx 4.6$ is shown enlarged and highlighted in Fig. 3(c). Again, periodic solutions are unstable along this entire branch. Finally, the third branch, shown enlarged and highlighted also in Fig. 3(c), bridges the self-intersection for $N \approx 4.15$. This third branch is the longest, starting at the Hopf bifurcation ($*$) that bounds the stability region of ECMs and connecting to a different Hopf bifurcation ($*$). The periodic orbits are initially stable (in the low-inversion region), but then lose their stability in a torus bifurcation ($\diamond$), which gives rise to quasiperiodic dynamics. The periodic orbits along this branch are shown in Fig. 4, which illustrates their dependence on the parameter $C_p$. Indeed, they start from a point, after a Hopf bifurcation of a stable ECM, are initially stable, lose their stability, and then shrink back to a point at another Hopf bifurcation.

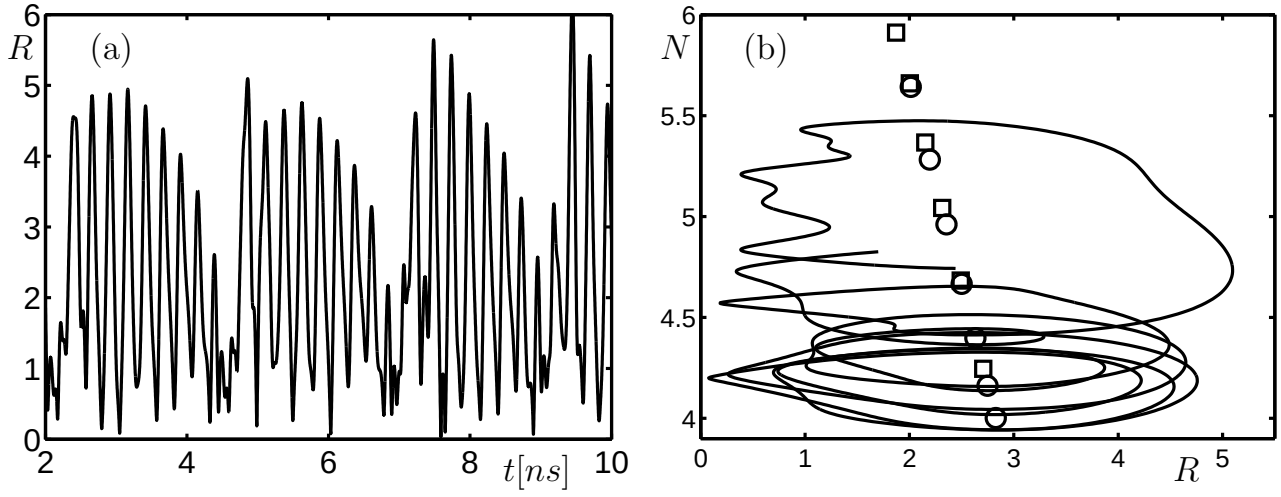


**Figure 5.** A time plot of pulse packages and the projection of a single pulse package on the $(R, N)$-plane; the plot is for $C_p = 20.10$.

## 4. COMPUTATION OF 1D UNSTABLE MANIFOLDS

To gain more insight into the global organization of the phase space we now compute 1D unstable manifolds of saddle ECMs. In the present situation these can be computed by integrating suitable initial conditions in the 1D unstable eigenspace of the respective ECM; see Ref. [16, 17] for more details of the method. For the purpose of this paper, it is sufficient to realize that these 1D unstable manifolds are one-dimensional curves in projection onto the $(R, N)$-plane, which essentially tell one how trajectories that come close to the respective ECM move away from it. By finding out where these curves end up one can gain important global information, for example, on the structure of basins of attraction. Finally, we mention that computing the 1D unstable manifolds of *all* relevant saddle-type ECMs (those with a positive real eigenvalue) constitutes a systematic method for finding attractors. In this way, all attractors that are 'connected' to ECMs will be found reliably. Note that this cannot be guaranteed by numerical integration from random initial conditions.

The connection between the time series and the phase space picture of a pulse package is made in Fig. 5. Panel (a) shows a time plot of several pulse packages, while panel (b) is the projection of a single pulse package onto the $(R, N)$-plane. Also shown in the $(R, N)$-plane are the ECMs. Notice that the trajectory corresponding to the pulse package starts near an ECM and first makes an excursion into the high-inversion region before being 're-injected' into the low-inversion region. Whenever the trajectory comes close to the $N$-axis in Fig. 5(b) the power drops, leading to the distinct pulses in Fig. 5(a). After the pulse package the trajectory is close to where it started. Since it does not repeat exactly, the next pulse package will look slightly different, while maintaining the main features.

To study the global features underlying the pulse packages we show in Fig. 6 the 1D unstable manifold of one of the ECMs during the entire $2\pi$-periodic transition. Specifically, the first column shows one branch of the manifold (which we refer to as the left branch), the second column the other (the right) branch, and the third column the attractor at which both branches end up. The ECMs are also shown in projection onto the $(R, N)$-plane, where circles correspond to modes and crosses to antimodes. The rows correspond to the same values of $C_p$ as were used for the time series in Fig. 1.

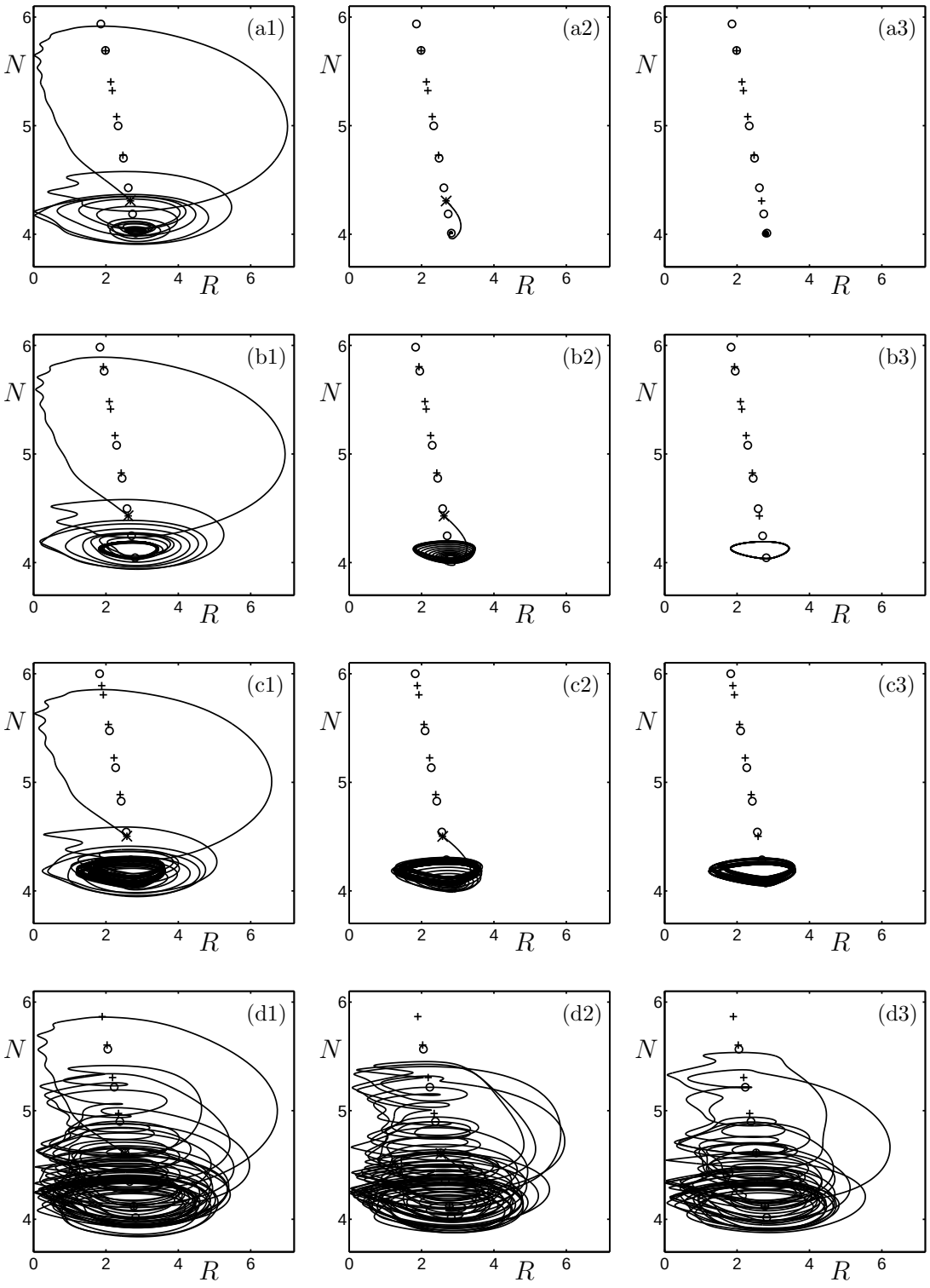


**Figure 6.** Left branch (first column) and right branch (second column) of the 1D unstable manifold of a saddle ECM. The attractor at which both branches end up is shown in the third column. From row (a) to row (d) the feedback phase $C_p$ takes the values 24.39, 22.74, 21.67, and 20.10.

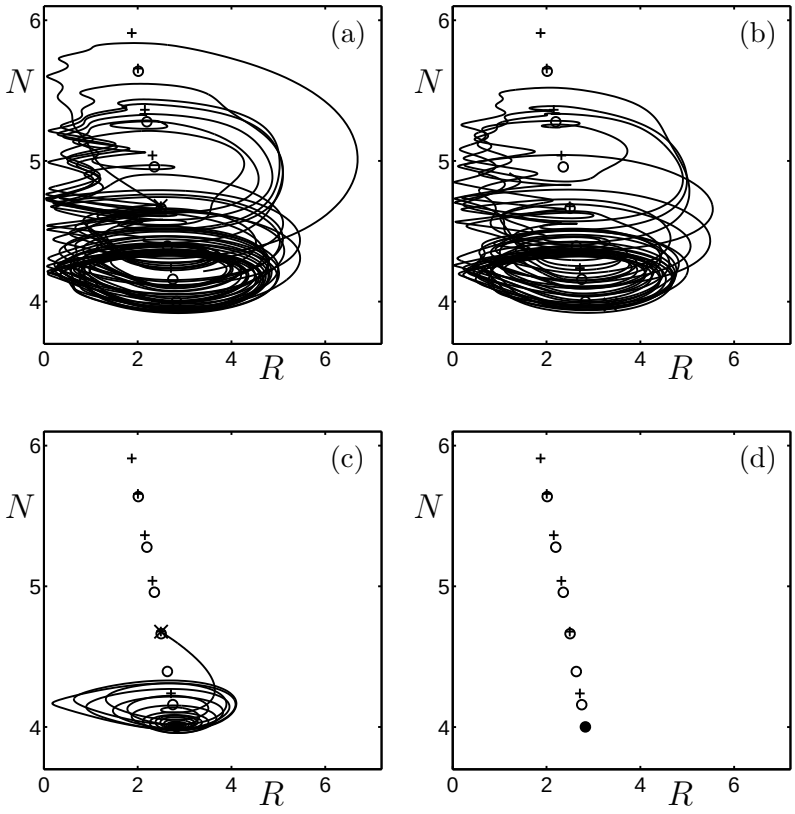


**Figure 7.** An example of bistability, where the left branch (a) ends up at a large attractor (b), while the right branch (c) ends up at an attracting ECM (d); the plots are for $C_p = 31.49$.

In row (a) of Fig. 6 both branches of the unstable manifold end up at a stable ECM, but the difference is that the left branch makes a large excursion into the high-inversion region before settling down to the ECM, while the right branch goes to this ECM straight away. This large excursion corresponds to transient behavior of the laser. The difference in the global features of the two branches can also be seen in rows (b) and (c), where the branches of the 1D unstable manifold go to a periodic orbit and a quasiperiodic torus, respectively. Finally, row (d) shows the case of pulse packages. Both branches end up at a complicated attractor shown in panel (d3). It is still the case that the left branch makes a global excursion, while the right branch first goes to the vicinity of the ECM with lowest inversion.

The creation of pulse packages can be interpreted as a successive 'inclusion' of more and more ECMs in the dynamics. This means that the 1D unstable manifolds of the saddle ECMs start to play a role. In fact, the large excursion of the left branch of the unstable manifold shown in the column (a) of Fig. 6 eventually becomes 'absorbed' into the attractor. At this stage, the pulse packages become quite regular, because the attractor needs to 'squeeze through' a narrow region defined by this first excursion; compare Fig. 5(b).

Finally, the pulse packages disappear in what is called a boundary crisis,[20] where the large complicated attractor collides with a saddle ECM. This bifurcation goes along with a bistability between a stable ECM and the pulse package attractor. Figure 7 shows an example of this bistability. The left branch of the stable manifold ends up at the pulse package attractor [see panels (a) and (b)], while the right branch ends up at the stable ECM [see panels (c) and (d)]. Notice that the left branch in Fig. 7(a) very much resembles that in Fig. 6(d1). When the stable ECM disappears in a saddle-node bifurcation, the right branch of the unstable manifold will come close to where the ECM was and will then also end up at the pulse package attractor. On the other hand, immediately after the boundary crisis the pulse package attractor disappears, and the left branch will settle down to the stable ECM only after a complicated transient.

## 5. CONCLUSIONS

The external cavity modes of the Lang-Kobayashi equations for the case of a laser with short conventional optical feedback were studied by means of numerical continuation. This revealed their dependence and stability as a function of the feedback phase. Periodic bridges are associated with self-intersections of the ECM curves in the plane of feedback phase versus inversion. The ECM structure constitutes the backbone of the $2\pi$-periodic dynamical scenario, involving the creation of pulse packages, that has been observed experimentally.[4,5]

Furthermore, we presented 1D unstable manifolds that show that complicated transients exist during the entire $2\pi$-periodic dynamical scenario. The creation of pulse packages can be described as an inclusion of more transients as the feedback phase is varied. The pulse packages finally disappear suddenly in a boundary crisis bifurcation and the laser settles back to constant output. The bifurcation study presented here is in good agreement with experimental measurements.[5]

The bifurcation scenario leading to pulse packages in the short cavity regime depends very strongly on the feedback phase $C_p$. This is so because the entire ellipse of external cavity modes is traversed by changing $C_p$ over a few multiples of $2\pi$ (owing to the relatively small number of ECMs). For a large cavity, on the other hand, there are typically several hundred or even thousands of ECMs, so that $C_p$ must be changed over several hundred or thousands of multiples of $2\pi$ in order to traverse the entire ellipse of ECMs. This explains why the feedback phase $C_p$, while still creating a $2\pi$-periodic bifurcation scenario, is not considered a crucial parameter in the long cavity regime.

Changing the length of the external cavity from a short to a long cavity gradually increases the number of ECMs and decreases the importance of $C_p$. The scenario leading to pulse packages discussed here can be seen as a precursor of more complicated dynamics, including low-frequency fluctuations and coherence collapse, which are the characterizing features of lasers with long external cavities. In this sense, the study of the short cavity laser also contributes to our understanding of dynamics and bifurcations in the long cavity regime, which remains a major challenge.

## REFERENCES


1. G. H. M. Van Tartwijk and G. P. Agrawal, "Laser instabilities: a modern perspective," *Prog. Quantum Electron.* **22**, pp. 43–122, 1998.
2. G. H. M. Van Tartwijk and D. Lenstra, "Semiconductor lasers with optical injection and feedback," *Quantum Semiclass. Opt.* **7**, pp. 87–143, 1995.
3. B. Krauskopf and D. Lenstra, eds., *Fundamental Issues of Nonlinear Laser Dynamics*, vol. 548, AIP Conf. Proc., 2000.
4. T. Heil, I. Fischer, W. Elsäßer, and A. Gavrielides, "Dynamics of semiconductor lasers subject to delayed optical feedback: The short cavity regime," *Phys. Rev. Lett.* **87**(243901), 2001.
5. T. Heil, I. Fischer, W. Elsäßer, B. Krauskopf, K. Green, and A. Gavrielides, "Delay dynamics of semiconductor lasers with short external cavities: Bifurcation scenarios and mechanisms," *Phys. Rev. E* **67**(066214), 2003.
6. A. Tabaka, M. Sciamanna, I. Veretennicoff, K. Panajotov, "Mapping of delayed dynamics in short external cavity", this volume: *Proceedings of SPIE* **5452**, 2004.
7. R. Lang and K. Kobayashi, "External optical feedback effects on semiconductor injection laser properties," *IEEE J. Quantum Electron.* **16**(3), pp. 347–355, 1980.
8. J. K. Hale and S. M. Verduyn Lunel, *Introduction to Functional Differential Equations*, Springer-Verlag, 1993.
9. O. Diekmann, S. A. Van Gils, S. M. V. Lunel, and H. O. Walther, *Delay Equations: Functional-, Complex-, and Nonlinear Analysis*, vol. 110, Springer-Verlag, 1995.
10. S. M. Verduyn Lunel and B. Krauskopf, "The mathematics of delay equations with an application to the Lang-Kobayashi equations," in Krauskopf and Lenstra,[3] pp. 66–86.
11. B. Krauskopf, G. H. M. Van Tartwijk, and G. R. Gray, "Symmetry properties of lasers subject to optical feedback," *Opt. Commun.* **177**, pp. 347–353, 2000.

12. K. Green, B. Krauskopf, and G. Samaey, "A two-parameter study of the locking region of a semiconductor laser subject to phase-conjugate feedback," *SIAM J. Dynamical Systems* **2**(2), pp. 254–276, 2003.
13. K. Green and B. Krauskopf, "Bifurcation analysis of a semiconductor laser subject to non-instantaneous phase-conjugate feedback," *Opt. Commun.* **231**, pp. 383–393, 2004.
14. D. Pieroux, T. Erneux, T. Luzyanina, and K. Engelborghs, "Interacting pairs of periodic solutions lead to tori in lasers subject to delayed feedback," *Phys. Rev. E* **63**(036211), 2001.
15. K. Engelborghs, T. Luzyanina, and G. Samaey, "DDE-BIFTOOL v2.00: a Matlab package for bifurcation analysis of delay differential equations," Tech. Rep. TW-330, Department of Computer Science, K. U. Leuven, Belgium, 2001. `http://www.cs.kuleuven.ac.be/~koen/delay/ddebiftool.shtml`.
16. B. Krauskopf and K. Green, "Computing unstable manifolds of periodic orbits in delay differential equations," *J. Comput. Phys.* **186**, pp. 230–249, 2003.
17. K. Green, B. Krauskopf, and D. Roose, "Software for computing unstable manifolds of delay differential equations", Technical Report **377**, K.U. Leuven, 2003.
18. D. Pieroux, T. Erneux, B. Haegeman, K. Engelborghs, and D. Roose, "Bridges of periodic solutions and tori in semiconductor lasers subject to delay," *Phys. Rev. Lett.* **87**(193901), 2001.
19. B. Haegeman, K. Engelborghs, D. Roose, D. Pieroux, and T. Erneux, "Stability and rupture of bifurcation bridges in semiconductor lasers subject to optical feedback," *Phys. Rev. E* **66**(046216), 2002. ).
20. C. Robert, K.T. Alligood, E. Ott, J.A. Yorke, "Explosions of chaotic sets," *Physica D* **144**, pp. 44–61, 2000.